Rev. Roum. Sci. Techn.– Électrotechn. et Énerg.
Vol. 66, 4, pp. 285–292, Bucarest, 2021

ESTIMATION AND MAPPING OF LINKE TURBIDITY FACTOR FROM SOLAR RADIATION MEASUREMENT FOR INDIAN CLIMATIC CONDITIONS

NEELAM RATHORE[1], NARAYAN LAL PANWAR[1], FATIHA YETTOU[2], AMOR GAMA[2]

Key words: Linke turbidity factor, Direct normal irradiation, Statistical analysis, Surfer software mapping, India.

For development, installation, and examining the performance of solar energy devices, it is necessary to have knowledge of solar radiation. Solar radiation gets attenuated by factors such as optical thickness, water content, and aerosols, etc. All these factors are expressed in terms of Linke turbidity (LT). In this study, an attempt is made to assess the Linke turbidity values through a calculative approach. Linke turbidity is a key input for several models that assess solar radiation under clear skies. The Linke turbidity for each month at every location of India was estimated using the MATLAB program. The value obtained from the MATLAB program was further validated by measured values taken from the SoDa site and Linke turbidity maps were generated using Surfer software. These generated maps show year around mean value of each Indian location. As observed from developed Linke turbidity maps, LT value is high in summer (April – June) and lower in winter (October – February). The value of LT lies in the range of 1 – 4.1 during the winter season while it increases to cover a range of 4.6 – 6 in the summer season.

1. INTRODUCTION

With a population of over one billion people, India is dealing with issues such as a rapidly rising economy and massive energy demand [1 – 3]. India, on the other hand, has a large solar potential, with 300 clear bright days a year. Harnessing available solar energy in efficient way can improve energy deficit scenario [4 – 6]. Even, the Indian Energy Portal predicted that if 10 % of the land were used for harnessing solar energy, the installed solar capacity would be at 8,000 GW, or around fifty times the current total installed power capacity in the country [7]. A number of initiatives have been taken by many government agencies to encourage the usage of solar energy technology for electricity production [8]. Therefore, in order to promote solar power, Government has launched National Solar Mission which aims at achieving total installed solar capacity of 100 GW by 2022 [9]. Consistent solar irradiation primarily require for optimal design and performance assessment of solar related energy conversion system like photovoltaic, solar thermal systems, *etc.* [10, 11]. Consecutively solar irradiation gets attenuated as it traverses from upper atmospheric layer to ground and absorbed at different wavelengths by numerous components in the different way. Physical properties and number of aerosols is used to determine the level of pollution and hence can give information on diffuse and direct solar radiation. Atmosphere is said to be turbid when aerosols are present in it. Aerosols present in the atmosphere make it turbid. Aerosols is having a radius of 10^{-3} to 102 μm [12]. It may be of terrestrial origin (industrial smoke, pollen, volcanic eruptions, meteoric dust, sandstorms, forest fires and agricultural and slash burning), or of marine origin (from salt crystals, ocean spray and nuclei of hygroscopic salt on which water has condensed). According to Iqbal (1983) rain and snow does not come under aerosols while water suspended particles along with fog lie on the borderline of the classification of aerosol particles [13] Turbidity produced by aerosols is expressed in factor called Linke turbidity factor. Elminir describe it as index of number of clear and dry atmospheres that would be necessary to produce the same attenuation of extra-terrestrial radiation as is produced by the real atmosphere [14] study of atmospheric turbidity is important for purposes of meteorology, ecology, climatology and monitoring of atmospheric pollution.

Solar radiation is scattered and absorbed by aerosol particles present in atmosphere [15]. Basically, the study of aerosols is done on a clear day when there is no cloud cover. A clear day has the clearness index between 0.7 and 0.9 [16]. The diffuse irradiation component gets altered by presence of clouds, which makes determining LT no more reliable. Therefore, overcast sky must not be considered while calculating LT [17]. Hence in this study, only clear days are considered.

India's solar potential is quite impressive. Solar radiation gets attenuated by factors such as optical thickness, water content, and aerosols, etc. Gases like ozone, carbon dioxide, water vapor and Sulphur dioxide absorb most of the radiation [18]. This attenuation is predicted by one common factor, *i.e.*, Linke turbidity, which is linked to the aerosols, that are basically gases, suspended particles in air. Aerosols and clouds attenuated the solar radiation when it passes through earth's atmosphere. It is observed that maximum radiation is achieved when aerosols are minimum and vice versa [14] . While installing photovoltaic (PV) and thermal system LT factor plays an important role. High value of LT factor indicates more diffuse radiation and less direct radiation. Therefore, solar photovoltaic system and concentrating solar thermal power generation system will be effective by an increase or decrease of LT factor. It is important to estimate the quantity of aerosols present as it affects the availability of solar radiation reaching to the earth surface. However, limited studies related to determining TL are available. Few studies gives value of atmospheric turbidity that too for only few sites [18] Only a few authors presented research on determining LT values, and they did so for nations other than India [19, 22]. Even several authors have addressed the unreliability of clear sky models when using average turbidity information rather

[1] Department of Renewable Energy Engineering, College of Technology and Engineering, Maharana Pratap University of Agriculture and Technology, Udaipur (Rajasthan) 313001, India, E-mail: neelamrathore79@gmail.com
[2] Unité de Recherche Appliquée en Energies Renouvelables, URAER, Centre de Développement des Energies Renouvelables, CDER, 47133, Ghardaïa, Algeria, E-mail: yettou.t@gmail.com

than locally obtained values. Thus the purpose of the study is to increase the knowledge on TL turbidity indices all over India which is helpful in determining the performance of photovoltaic and solar heating systems, Thus, maps of monthly mean values of Linke turbidity factors are generated for all India's territory using Surfer software based on SODA project data [23]. The monthly variation of LT on representative maps are validated with a calculative approach using developed MATLAB program based on long-term measurements of solar radiation (covering a period of 10 years).

2. NECESSITY TO DETERMINE LINKE TURBIDITY FACTOR

The atmospheric turbidity has great importance in climatology, in pollution studies and to predict the potential of solar energy [24]. An increase in LT value testifies increase in level of pollution at that place [25]. For selecting a site for installation of solar PV system and concentrating solar power systems, data of solar irradiation is necessary, which get attenuated by atmosphere. As a result, this attenuation factor must be computed correctly. Aerosol particles have a direct impact on the direct normal irradiance (DNI), which is a vital component for constructing concentrating power plants. In general, the local diffuse horizontal irradiance (DHI) get increased and DNI decreases by the increase in scattering caused by aerosols under clear skies [26]. Mostly concentrating solar system are projected in arid or desert areas as these areas have low cloudiness. While predicting accurate direct normal irradiation, Linke turbidity is an essential input. Gueymard presented review of 24 models for predicting relation for determining clear sky DNI with respect to Linke turbidity addressing several critical issues including: instrument error, impact of model performance, propagation of errors due to incorrect perceptible water, elimination of cloudy conditions [27].

3. DATA COLLECTION

Average monthly data for direct normal irradiance (DNI) from year 2006 to 2013 was collected from Indian Meteorological Department (IMD). IMD provided solar radiation data for all weather conditions, but after analyzing data clear sky were selected for consideration. Because Linke turbidity is computed for clear skies, the acquired data was filtered to only include values that corresponded to clear skies.

4. DETERMINATION OF LINKE TURBIDITY: METHODOLOGY

To determine the Linke turbidity a calculative approach was used as described by Marif [19]. Solar radiation is mainly influenced by Linke turbidity Factor (LTF), and it specifies scattering and atmospheric absorption of solar radiation under clear sky. Atmospheric optical densities in clean, dry, humid, and hazy conditions are indicated by this factor. In other words, LTF is the number of clean dry air masses that would result in the same extinction then real hazy and humid air [28]. Its value varies with locations; however, the differences are correlated with altitude.

There are numbers of models available, which can be used to determine Linke turbidity. However, Louche model is globally used for its higher efficient results [29]. Therefore, in the present study Louche equation was used to determine LT. Louche equation requires DNI, Solar constant, Rayleigh optical thickness and optical air mass as an input to determining LT. Therefore, this model is adopted for calculations [29]:

$$I_N = I_O \cdot \varepsilon \cdot \exp\left(-T_L \cdot m_A \cdot \delta_R\right) \tag{1}$$

Therefore, TL can be found out using solar constant (I_0), Direct Normal Irradiation (IN), relative optical air mass (m_A) and Rayleigh's optical thickness (δ_R):

$$T_L = \frac{\ln I_O - \ln I_N + \ln \varepsilon}{m_A \cdot \delta_R}, \tag{2}$$

where δ_R is Rayleigh's optical thickness, which is optical thickness of a pure Rayleigh scattering atmosphere, per unit area mass along a specified path length; I_0 is solar constant = 1 367 W/m² [28]; m_A is the relative optical air mass, which depends on Zenith angle θ_z and actual pressure at place.

Calculation of LT requires calculation of solar declination, solar hour angle, solar elevation angle, relative optical air mass and extra-terrestrial solar radiation. Therefore following equations are used for calculating LT [30]. Calculation of solar declination can be done using below mentioned:

$$\begin{aligned} &\sin(\delta) = \\ &= 0.3978 \cdot \sin\left[N_p - 1.4 + 0.0355 \cdot \sin\left(N_p - 0.0489\right)\right], \end{aligned} \tag{3}$$

with: $$N_p = 2 \cdot \pi \cdot N / 365.25. \tag{4}$$

Calculation of solar hour angle can be done by

$$\omega = 0.261799 \cdot (t - 12). \tag{5}$$

Solar elevation angle can be done using latitude, hour angle, declination angle:

$$\sin(\gamma_s) = \cos(\varphi) \cdot \cos(\delta) \cdot \cos(\omega) + \sin(\varphi) \cdot \sin(\delta), \tag{6}$$

where δ is declination angle, φ is latitude of place and ω is hour angle.

Calculation of relative optical air mass was done using

$$m_A = \frac{p/p_0}{\sin\left(\gamma_s^{cor}\right) + 0.50572 \cdot \left(\gamma_s^{cor} + 6.07995\right)^{-1.6364}} \tag{7}$$

The p/p_0 component in eq. (7) is correction for given elevation z [m]:

$$p/p_0 = \exp(-z/8434.5). \tag{8}$$

Calculation of integral Rayleigh optical thickness depending on its value can be done by:

- if $m_A \le 20$

$$\begin{aligned} (\delta_R)^{-1} &= 6.6296 + (1.7513 \cdot m_A) - \left(0.1202 \cdot m_A^2\right) + \\ &+ \left(0.0065 \cdot m_A^3\right) - \left(0.00013 \cdot m_A^4\right), \end{aligned} \tag{9}$$

- if $m_A > 20$

$$(\delta_R)^{-1} = 10.4 + (0.718 \cdot m_A). \tag{10}$$

The calculation of extra-terrestrial solar radiation G_0 was done using:

$$G_o = I_o \cdot \left[1 + 0.03344 \cos\left(j' - 0.048869\right)\right], \qquad (11)$$

where the day angle *j*' is in radians and *N* is the day number.

The calculation of DNI (W/m²) from direct radiation IB (W/m²) can be calculated using:

$$\mathrm{IN} = \mathrm{IB}/\sin\left(\gamma_s\right). \qquad (12)$$

Hence after the calculation of various affecting parameters Linke turbidity factor was calculated by:

$$T_L = \frac{1}{\left(m_A \cdot \delta_R\right)} \cdot \ln\left(\frac{I_O \cdot \varepsilon}{I_N}\right). \qquad (13)$$

To ease the calculation method, eq. (1) to eq. (13) was programmed in MATLAB to calculate T_L at any location, and program works as depicted through flowchart (Fig. 1), with successful execution of MATLAB program LT file was attained as an output file. This file is given as one of the inputs for Surfer software. Surfer software was used to create turbidity maps for the entire year in India. Surfer is a grid-based mapping program that interpolates irregularly spaced *XYZ* data into a regularly spaced grid. The application of Surfer is to create a grid-based map from an *XYZ* data file. Surfer software needs 3 files for creating a grid file, *i.e.*, latitude file, longitude file and elevation file of India. Latitude file consists of 8°4' to 37°6' North, which further includes loop to increment longitude value from 68°7' to 97°25' East. The Data command requires three columns of data: one column for latitude, one column for longitude, and one column for elevation. Following the entry of a grid file and a Linke turbidity file, contour maps were generated.

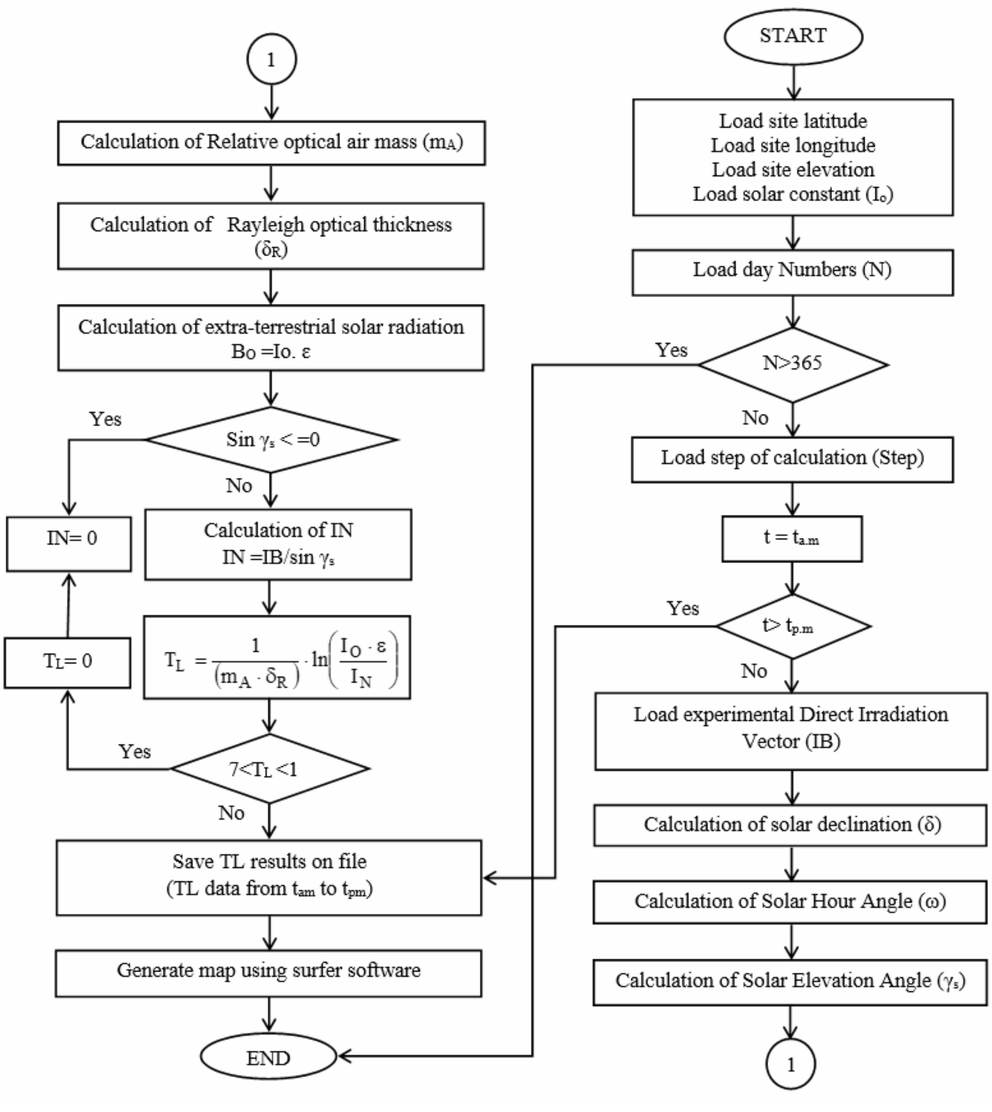

Fig. 1 – Flow chart for calculating T_L factor using MATLAB program.

5. **RESULTS AND DISCUSSIONS**

Louche Linke turbidity model is function of direct normal irradiance, Rayleigh's optical thickness, and Rayleigh scattering atmosphere. Linke turbidity for clear sky was calculated from above equations using various parameters for eight years, *i.e.*, 2006 to 2008 for all the Indian states as direct radiation was used as provided by IMD.

5.1. VALIDATION

To perform validation, calculated values of LT were compared with measured value. Solar Radiation Data

(SoDa project website) was used for measuring Linke turbidity values. SoDa uses photos from Meteosat geostationary satellites to give real-time and forecast LT values. Values taken from SoDa site were considered as measured values. SoDa website needs latitude, longitude, and elevation of location for measuring Linke turbidity values for the whole year. Calculated LT value was compared with measured value from SoDa site. Locations like Jaipur, Kolkata, New Delhi, and Mumbai were selected for performing validation. Calculated LT values for all 4 cities were compared from measured values. Graphs were plotted to determine errors for 4 locations as shown in Fig. 2. To increase the confidence in the calculated values, statistical analysis was also performed to check errors.

The root mean square error RMSE indicator

$$\mathrm{RMSE} = \frac{1}{m}\sqrt{\frac{1}{n}\sum_{i=1}^{n} e_i^2}\,, \tag{14}$$

where n is number of measured and computed values, denoted by m_i and n_i (i = 1 to n), respectively

$$e_i = m_i - c_i, \tag{15}$$

was used to determine accuracy (Table 1). The mean value of measured values is given by

$$m = \frac{1}{n}\sum_{i=1}^{n} m_i\,. \tag{16}$$

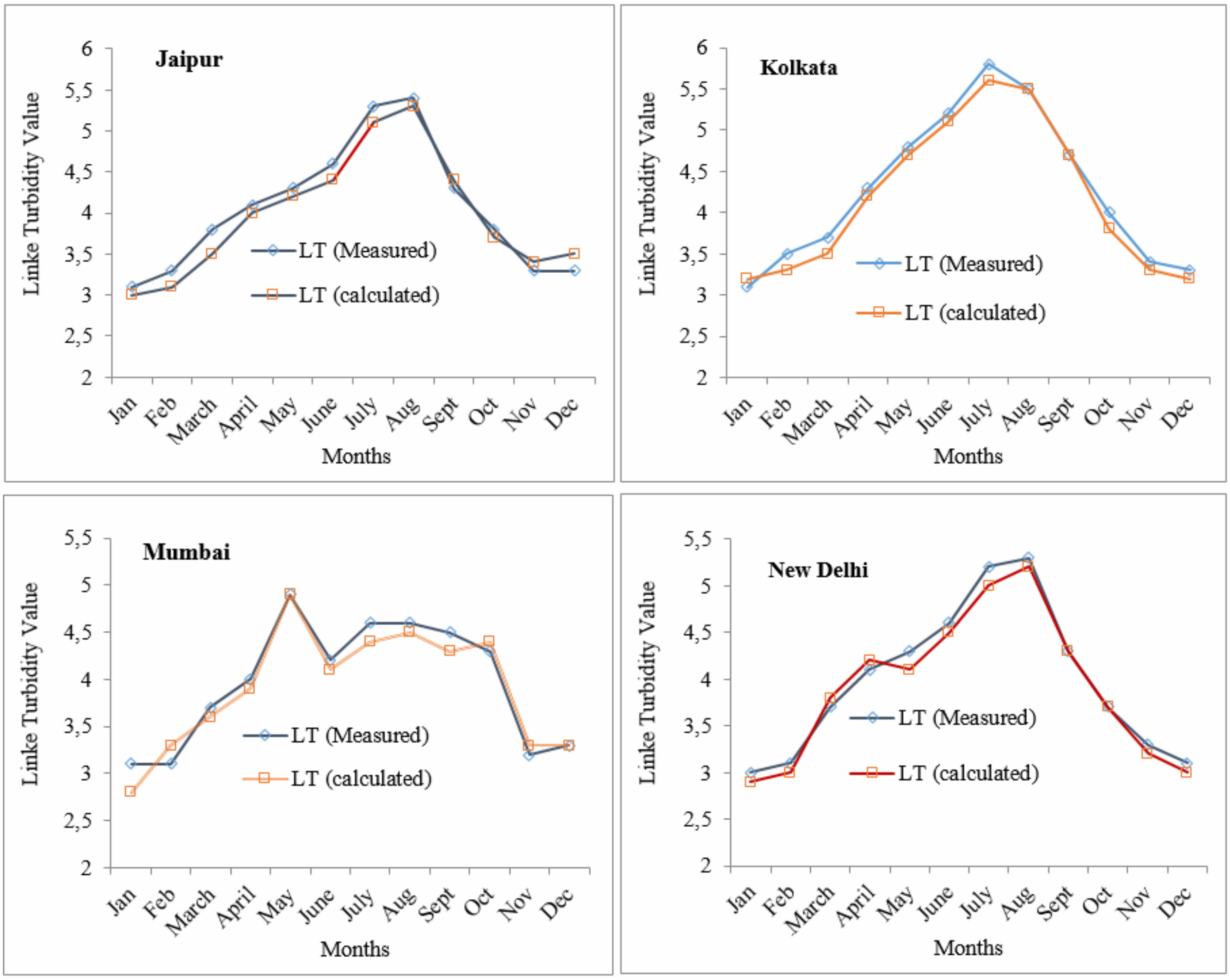

Fig. 2 – Validation graph between measured and calculated LT values.

Table 1

RMSE values for different location of India

Location	RMSE (%)
Jaipur	0.60
Mumbai	0.87
Kolkata	0.78
New Delhi	0.75

If RMSE lies in range of 0,1-1,0, it specifies good agreement between calculated and measured values as suggested by [31]. Therefore, the above calculative approach can be used to determine LT for any place in India.

5.2. LINKE TURBIDITY FILE

Since it is difficult to know which observation is closer to truth, averages of two values were used for mapping purpose. Finding minimum error between calculated and measured values, a file consisting of mean Linke turbidity value for whole India at every location was created. Mean values, *i.e.*, average values between measured and calculated values were considered as an input file for Surfer software. As a result, the maps generated depict average LT values for India as a whole.

5.3. MAPS OF LINKE TURBIDITY

Maps of LT were generated after verification and performing error analysis (Fig. 3 to Fig. 14). As observed from various Linke turbidity maps, LT value is high in summer (April – June) and lower in winter (October – March). The value of LT lies in range of 1 – 4.1 during winter season while it increases to cover range of 4 – 6 in summers. Table 2 shows some parameters indicators for various degrees of atmospheric cleanliness.

Table 2

Parameters for various degrees of atmospheric cleanliness [32]

Atmosphere	Linke turbidity	Visibility (km)
Pure Rayleigh Atmosphere	1	340
Clean, warm air	2	28
Turbid, moist, warm air	3–4.1	11
Polluted atmosphere	4.2–6	< 5

Seasonal variation: India has three seasons: winter from October to March, hot summer from April to June, rainy season: July to September. As the season changes there is change in daytime temperature and prevailing winds.

Linke turbidity maps for winter season from month October to March are shown in Fig. 3 to Fig. 8. It can be observed that LT is lower in winter season. Winter is followed by low aerosol concentration and passage of western disturbances. Low aerosol content accounts due to lower temperature inversion. Turbidity is lower in winter season due to absence of dust and desert storm. As a result, the chilly and less humid climate remains during the winter season. Linke turbidity is a significant metric for assessing air pollution, as well as the key control parameter for the reduction of solar radiation reaching the earth's surface under clear skies.

As observed in all maps of winter season (Fig. 3 to Fig. 8), southern states like Karnataka, Tamil Nadu, Kerala receives maximum LT in winter season. Linke turbidity is lowest in states like Jammu & Kashmir and Arunachal Pradesh. LT value increases in states like Rajasthan, New Delhi, and Bihar. Direct normal irradiance has logarithmic relation with LTF while diffuse irradiation is directly proportional to LTF. States having high vales of Linke turbidity will have high value of diffuse irradiation.

Summer season is observed in India during April to June months. While Linke turbidity is higher in summer months in range of 4–6 due to existence of high dust storm and high particle flux. Atmosphere convection increases due to higher temperature inversion is summer season. LT maps for summer season are shown in Fig. 9 to Fig. 11. DNI which is a critical component for developing concentrating power plant is directly influenced by aerosol particles. In general, the local Diffuse Horizontal Irradiance (DHI) gets increased and DNI decreases by the increase in scattering caused by aerosols under clear skies. Mostly concentrating solar system is projected in arid or desert areas as these areas have low cloudiness. When it comes to forecasting the irradiance of direct normal irradiation with accuracy, the input of Linke turbidity is critical.

The observed values are lower than the previous values presented by Narain and Garg [18], due to the reason that in this study only clear sky days are considered. The study done by Narain and Garg presented LT values for all days (cloudy and clear days). Linke turbidity for summer season lies in range of 4.6 to 6, which shows major portion of India is polluted [32].

LT maps for monsoon season are as shown in Fig. 12 to Fig. 14. The temperature of surface drops from pre monsoon to monsoon season. Increase in cloudiness is observed in summer Monsoon. In upper troposphere temperature gradient is higher as compared to lower troposphere. Pre-Monsoon season is marked by clear sky and increase in solar radiation and hence increase in Linke turbidity value. LT values are high in rainy season showing peak in August. More is value of LT; less is value of clearness index. High value in August leads to trapping of pollution in boundary layer, causing environmental problems. High Linke turbidity also accounts for increase in diffuse irradiation. More Increased turbidity causes an increase in aerosol particles, which scatter light more and hence enhance diffuse irradiation. It can be seen from various maps that LT is highest in these months which increases turbidity of air and decreases the visibility, hence affect environmental quality of cities. The higher the value of LT, the more solar radiation will be scattered and absorbed.

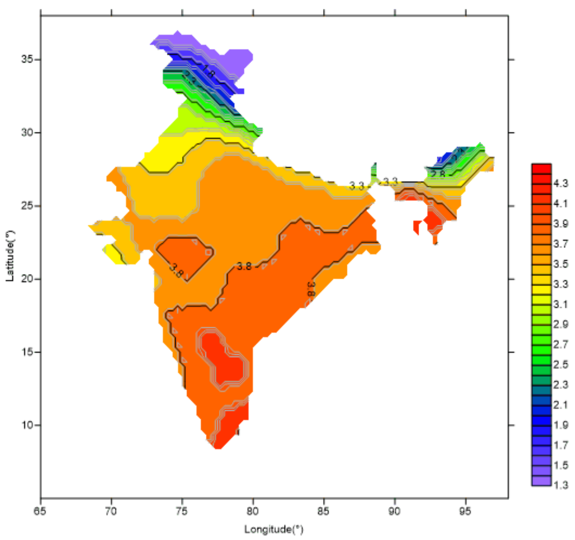

Fig. 3 – LT map of October month over India.

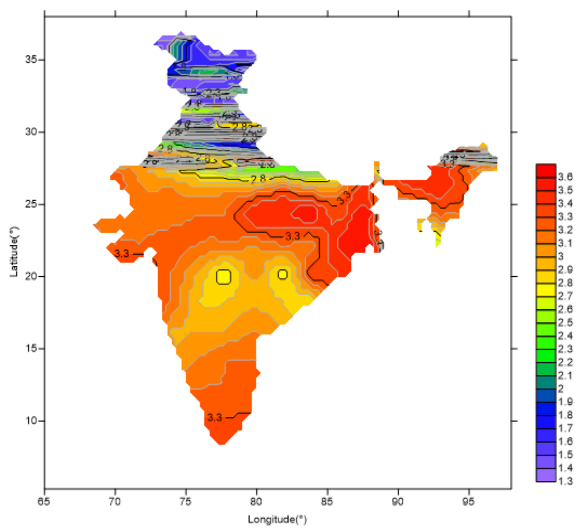

Fig. 4 – LT map of November month over India.

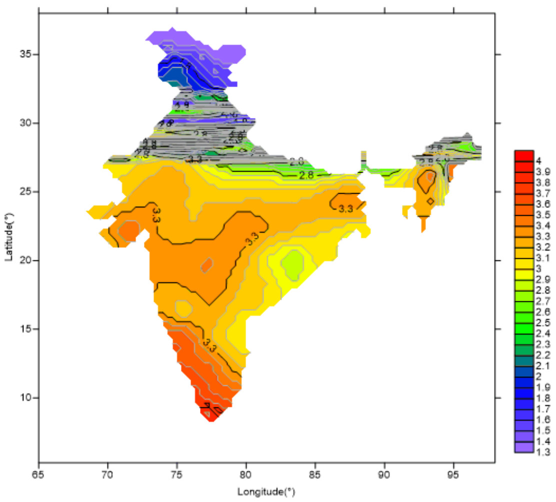

Fig. 5 – LT map of December month over India.

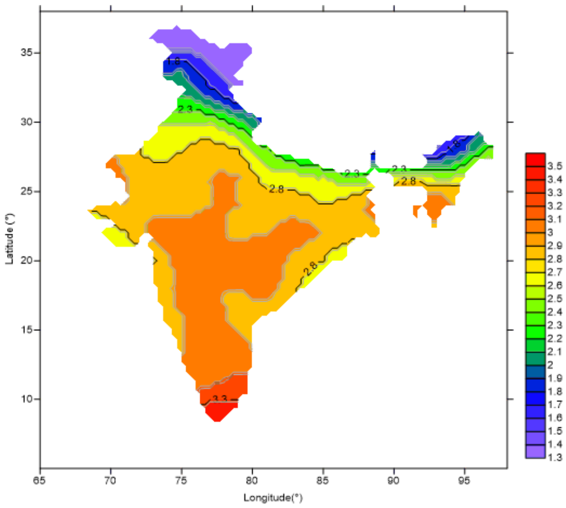

Fig. 6 – LT map of January month over India.

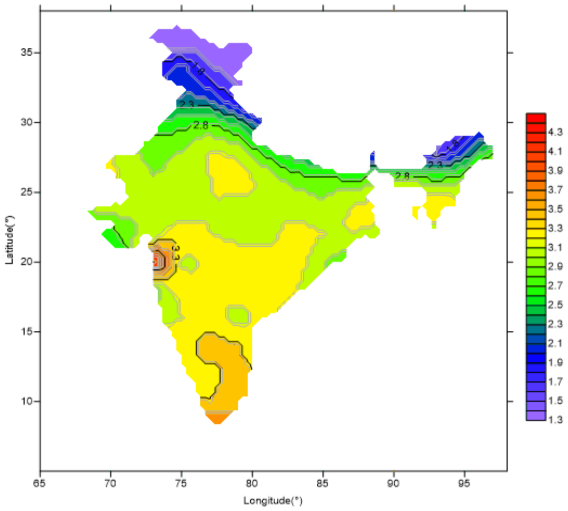

Fig. 7 – LT map of February month over India.

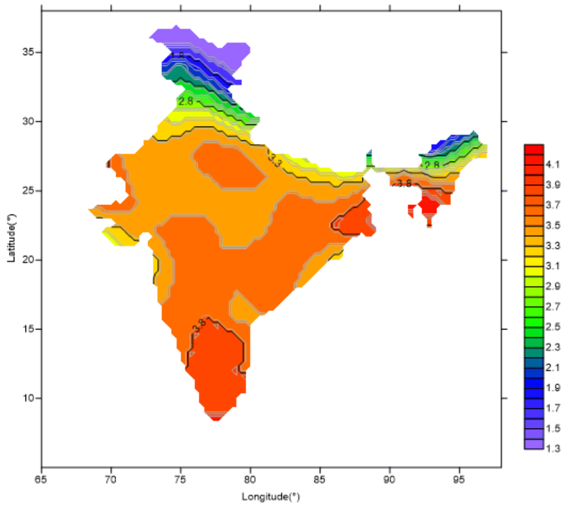

Fig. 8 – LT map of March month over India.

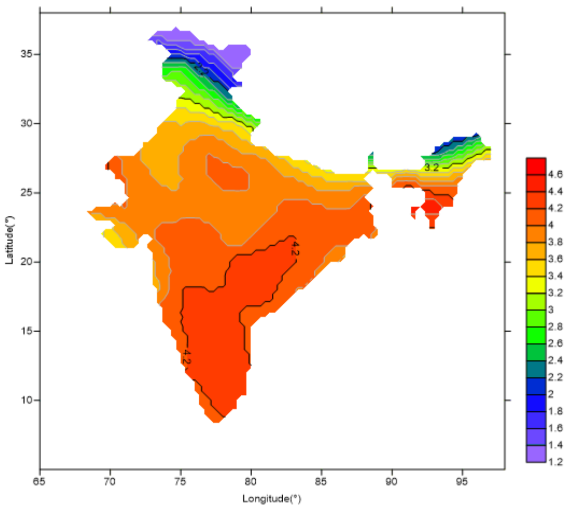

Fig. 9 – LT map of April month over India.

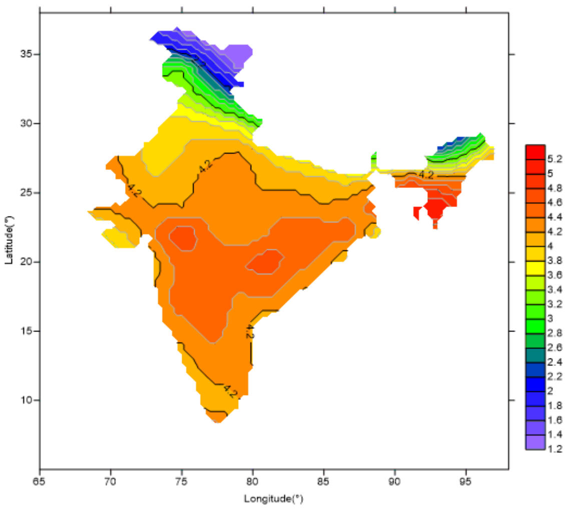

Fig. 10 – LT map of May month over India.

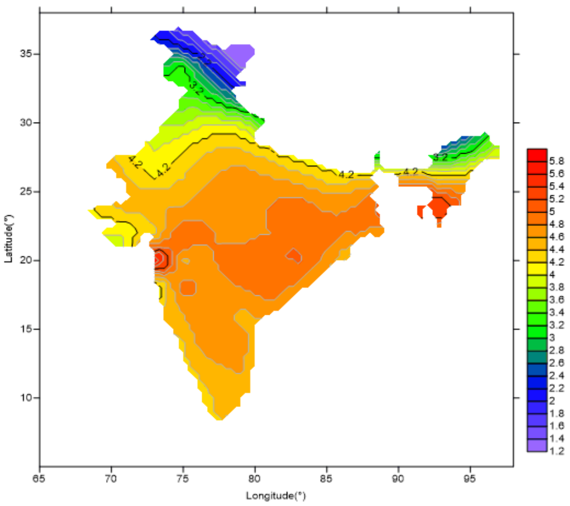

Fig. 11 – LT map of June month over India.

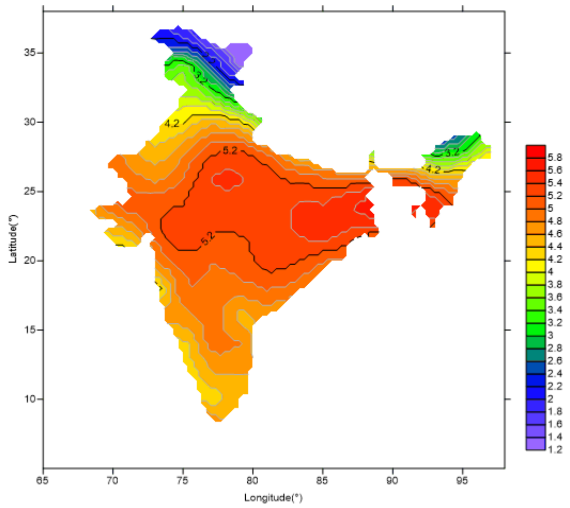

Fig. 12 – LT map of July month over India.

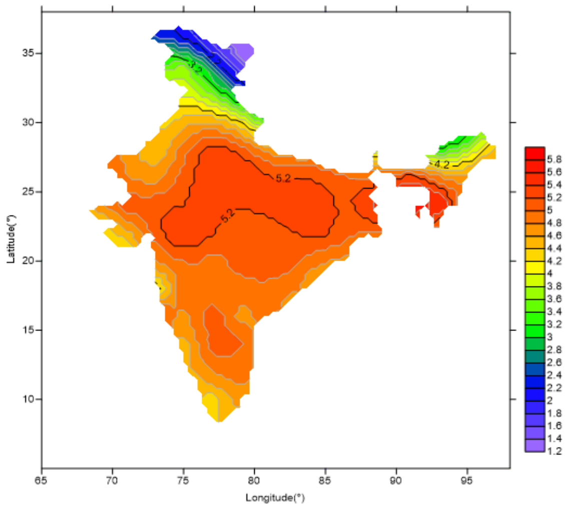

Fig. 13 – LT map of August month over India.

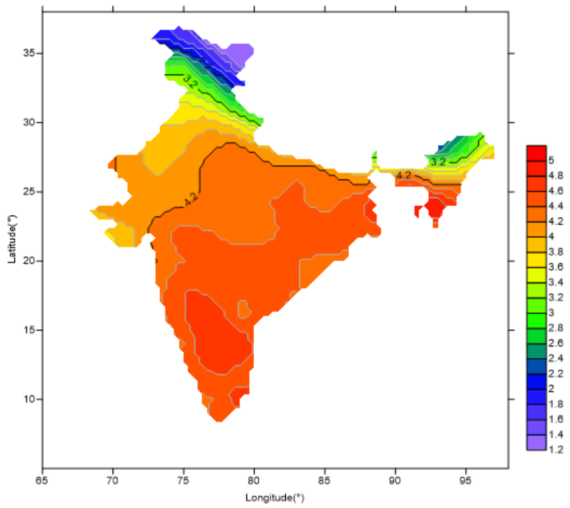

Fig. 14 – LT map of September month over India.

6. CONCLUSIONS

This work proposed model for determining LT from DNI for clear sky conditions. No information is available related to LTF for clear sky in Indian climatic conditions. Therefore, this developed model calculates LTF for clear sky in Indian climatic conditions and hence maps are generated which presents LT values at every location. LT values were than validated by values measured by SoDa site. Error analysis was also performed between measured and calculated values. RMSE and MBE were found in permissible range. LT value is high in summer (4.6 – 6) and lower in winter (1 – 4.1) as observed by generated maps. Further the Linke turbidity factor is of specific importance for the calculation of beam and diffuse solar radiation in a determined locality. Thus, it is important to determine LT values before installing any solar PV and solar concentrating power plant. Therefore, atmospheric turbidity is not only an important factor for monitoring the air pollution, but it is significant in meteorology, climatology and for designing of solar energy systems.

Received on January 31, 2020

REFERENCES

1. S.L. Narnaware, N.L. Panwar, *Catalysts and their role in biomass gasification and tar abetment: a review*, Biomass Conversion and Biorefinery, Oct. 2021.
2. M. More, C. Agrawal, D. Sharma, N. Rathore, K. Samar, *Development of pellet machine for utilization of biogas slurry*, Advances in Engineering Design, Select Proceedings of ICOIED 2020, Springer, pp. 509–519, 2021.
3. M. R. Patel, N. Rathore, N. L. Panwar, *Influences of biochar in biomethanation and CO2 mitigation potential*, Biomass Conversion and Biorefinery, 2021.
4. M.Q. Duong, N.T.N. Tran, G.N. Sava, V. Tanasiev, *Design, performance and economic efficiency analysis of the photovoltaic rooftop system*, Rev. Roum. Sci. Techn.– Électrotechn. et Énerg., **64**, pp. 229–234, 2019.
5. P.S.P. Sikder, N. Patro, K. Sunil, *A modeling of stand-alone solar photo-voltaic system for rural electrification purposes*, Rev. Roum. Sci. Techn.– Électrotechn. et Énerg., **64**, pp. 241–246, 2019.
6. M.O. Benaissa, S. Hadjeri, S.A. Zidi, Y.I.D. Kobibi, *Photovoltaic solar farm with high dynamic performance artificial intelligence based on maximum power point tracking working as STATCOM*, Rev. Roum. Sci. Techn.– Électrotechn. et Énerg., **63**, pp. 156-161, 2018.
7. N. Rathore, N.L. Panwar, *Strategic overview of management of future solar photovoltaic panel waste generation in the Indian context*, Waste Management & Research: The Journal for a Sustainable Circular Economy, p. 0734242X2110039, Apr. 2021.
8. N. Rathore, N.L. Panwar, A. Gama, F. Yettou, *Solar map of India under clear sky conditions*, Int. J. of Sustainable Energy, **38**, 5, 2019.

9. N. Rathore, V.S. Sankhla, *Techno economic and life cycle assessment of 1 MW solar parabolic trough system for Udaipur zone*, Advances in Materials Processing and Manufacturing Applications, Springer, pp. 549–561, 2021.
10. K. Sharma, S. Kothari, N.L. Panwar, N. Rathore, K. Samar, *Experimental Investigation on farmer-friendly hybrid dryer for indoor drying of mushroom*, **2**, Advances in Energy Research, pp. 81–92, Springer, 2020.
11. K. Sharma, S. Kothari, N. L. Panwar, N. Rathore, *Design and development of solar energy powered maize milling machine*, International Journal of Ambient Energy, 2020.
12. A. C, *Determination of Linke's turbidity factors from model and measure solar radiations in the tropics over highland of south-east Ethiopia*, Journal of Earth Science & Climatic Change, **9**, *7*, 2018.
13. J. Pérez-Díaz *et al*., *Fogs: Physical basis, characteristic properties, and impacts on the environment and human health*, Water, **9**, *10*, p. 807, Oct. 2017.
14. H. K. Elminir, U.A. Rahuma, V. Benda, *Comparison Between Atmospheric Turbidity Coefficients of Desert and Temperate Climates*, Acta Polytechnica, **41**, *2*, 2001.
15. P. Ineichen, *Conversion function between the Linke turbidity and the atmospheric water vapor and aerosol content*, Solar Energy, **82**, *11*, pp. 1095–1097, 2008.
16. T. Hove, E. Manyumbu, *Estimates of the Linke turbidity factor over Zimbabwe using ground-measured clear-sky global solar radiation and sunshine records based on a modified ESRA clear-sky model approac*h, Renewable Energy, **52**, pp. 190–196, 2013.
17. L. Coste, E. Eftimie, *Linke turbidity modelling for Brasov urban Area*, Renewable Energy and Power Quality Journal, **1**, *8*, pp. 455-460, 2010.
18. L. Narain, S.N. Garg, *Estimation of Linke turbidity factors for different regions of India*, International Journal of Environment and Waste Management, **12**, *1*, p. 52, 2013.
19. Y. Marif, D. Bechki, H. Bouguettaia, M. Zerrouki, M. M. Belhadj, *Determination of Linke turbidity factor from solar radiation measurement in Adrar city*, International Renewable and Sustainable Energy Conference (IRSEC), Nov. 2016, pp. 183-186.
20. M. Zaiani *et al*., *Study of Atmospheric Turbidity in a Northern Tropical Region Using Models and Measurements of Global Solar Radiation*, Remote Sensing, **13**, 12, p. 2271, 2021.
21. L. Wang, Y. Chen, Y. Niu, G. A. Salazar, W. Gong, *Analysis of atmospheric turbidity in clear skies at Wuhan, Central China*, Journal of Earth Science, **28**, *4*, pp. 729-738, 2017.
22. D. Djafer, A. Irbah, *Estimation of atmospheric turbidity over Ghardaïa city*, Atmospheric Research, **128**, pp. 76–84, 2013.
23. Solar radiation data. http://www.soda-pro.com/web-ervices/atmosphere/linke-turbidity-factor-ozone-water-vapor-and-ngstroembeta.
24. M. Chaâbane, *Analysis of the atmospheric turbidity levels at two Tunisian sites*, Atmospheric Research, **87**, *2*, pp. 136-146, Feb. 2008.
25. S. Pashiaridis, S.A. Kalogirou, A. Pelengaris, *Statistical analysis and intercomparison of Linke turbidity factor for two sites in Cyprus: Athalassa (inland location) and Larnaca (coastal location)*, SM Journal of Biometrics & Biostatistics, **3**, *2*, 2018, [Online]. Available: https://www.jsmcentral.org/sm-biometrics-biostatistics/fulltext_mjbb-v3-1029.pdf.
26. R.H. Inman, J.G. Edson, C.F.M. Coimbra, *Impact of local broadband turbidity estimation on forecasting of clear sky direct normal irradiance*, Solar Energy, **117**, pp. 125-138, 2015.
27. C.A. Gueymard, J.A. Ruiz-Arias, *Validation of direct normal irradiance predictions under arid conditions: A review of radiative models and their turbidity-dependent performance*, Renewable and Sustainable Energy Reviews, **45**, pp. 379–396, 2015.
28. J. Hofierka, M. Suri, *The solar radiation model for open-source GIS: implementation and applications*, Open-source GIS - GRASS users Conference 2002, Trento, Italy, 11-13 September 2002.
29. A. Louche, G. Peri, M. Iqbal, *An analysis of Linke turbidity factor*, Solar Energy, 37, *6*, pp. 393-96, 1986.
30. N. Rathore, N.L. Panwar, F. Yettou, A. Gama, *A comprehensive review of different types of solar photovoltaic cells and their applications*, International Journal of Ambient Energy, 2019.
31. J. Remund, L. Wald, M. Lefèvre, T. Ranchin, *Worldwide Linke turbidity information*, ISES Solar World Congress 2003, Göteborg, Sweden 2003.
32. Rahoma, *Determination of atmospheric turbidity and its correlation with climatological parameters*, American Journal of Environmental Sciences, **8**, *6*, pp. 597-604, 2012.